Synthesis, Characterization, DFT Study and Antibacterial Studies of Co(II) complexes of thiosemicarbazide with Fructose and Glucose.

Rania .A. Abokhater[1] , Shafya.A.Aldenfaria[2] , Aisha .A.abudabbus[3]
Microbiology Department, Faculty of Medical Technology, Misurata, Libya[1,3]
Physics Department, Faculty of science, Misurata university, Libya[2]
mmahammed.77@gmail.com

تاريخ الاستلام 2024-10-12

الملخص

تتناول الدراسة الحالية دراسات تجريبية وحسابية مشتركة على معقدات الكوبلت (II) والمهام الطيفية . المعقدات المحضرة صيغتها العامة [Co (TSC) (FRU)] (A1) ‏ [Co (TSC) (GLU)] (A2), حيث (FRU) هو الفركتوز (GLU) هو الجلوكوز و (TSC) ثيوسيميكاربازيد تم تصنيعه في خطوتين . تتم إضافة TSC كمركب ترابط ثانوي بعد تفاعل [$CoCl_2.6H_2O$]مع الفركتوز أو الجلوكوز باعتباره المركب الابتدائي , تم ربط FRU و GLU و TSC بالمركز المعدني ل Co(II) في الهياكل المقترحة , كذلك تم استخدام تقنيات الأشعة فوق البنفسجية المرئية (UV-Vis) لفحص الخصائص الطيفية للمعقدات . تم العثور على المنطقة بين 4000 و 600 سم$^{-1}$ لتمثل التخصيص الاهتزازي التفصيلي لطيف FT-IR المرصود في الحالة الصلبة , بالإضافة إلى ذلك تم استخدام حسابات نظريه الكثافة الوظيفية (DFT) التي تستخدم B3LYP ، تم استخدام مجموعة أساس وظيفيه هجينه مع 6–311++G (d, p) لذرات (H , C , N , F , O and Cl) من العوامل المخلبية لدراسة الخواص الفيزيائية والكيميائية الكميه في المعقدات المعدنية المحضرة باستخدام حزمة برنامج Gaussian 09, بالإضافة إلى ذلك ، تم اختبار المعقدات الجديدة ضد الأنواع المضادة للبكتريا التالية : Staphylococcus aureus , Streptococcus spp , Escherichia coli , Klebsiella spp , Pseudomonas spp and Protues spp.

وفقاً للنتائج فإن المعقدات الجديدة تمنع بشكل فعال نمو الكائنات الحية الدقيقة المسببة للأمراض المختارة بتركيزات عالية.

الكلمات المفتاحية: مضادات البكتريا ، كلوريد الكوبلت الثنائي ، فركتور، جلوكوز ، تخليق ، ثيوسيمكاربازيد

ABSTRACT

The current study reports combined experimental and computational studies on cobalt (II) complexes molecular structure and spectroscopic assignments. Complexes of the general formulas [Co (TSC) (FRU)] (A1), [Co (TSC) (GLU)] (A2), (where (FRU) is Fructose ,(GLU) is Glucose, and (TSC) is thiosemicarbazide) were synthesized in two steps. TSC is added as a secondary ligand after the reaction of [$CoCl_2$.6H2O] with either FRU or GLU as the primary ligand. The FRU or GLU and (TSC) ligands are attached to the Co(II) metal center in the proposed structures. UV-Vis techniques were used to investigate the complexes spectroscopic features. The region between 4000 and 600 cm^{-1} represented the detailed vibrational assignment for the observed FT-IR spectrum in the solid state. Using Density functional theory (DFT) calculations employing B3LYP, hybrid functional together with 6–311++G (d, p) basis set for atoms (H, C, N, F, O and Cl) of chelating agents were used to study the quantum physical and chemical properties of the synthesized metal complexes using the Gaussian 09 program package, the new complexes were tested against the following antibacterial types : Staphylococcus aureus , Streptococcus spp , Escherichia coli , Klebsiella spp , Pseudomonas spp and Proteus spp. According to the findings, the new compounds effectively inhibited the growth of the chosen pathogenic microorganisms at high concentrations .

Keywords: *Synthesis* , DFT , *Antibacterial* , Co(II) complexes *thiosemicarbazide* , *Fructose* , *Glucose*

1. Introduction

Thiosemicarbazones are used in various ways, including the coordination of neutral or deprotonated forms, their versatility, and the donor atoms of ligands (Abdel-Rahman *et al*., 2017). Chelation ligands known as thiosemicarbazones and their complexes are helpful tools for a range of bioinorganic processes (Berto *et al*., 2019;CAKMAK *et al*., 2013) Thiosemicarbazones commonly act as bidentate ligand through nitrogen and sulphur atoms(Deodware *et al*., 2022).

synthesis and characterization of mixed ligand coordinating Co(II), Cu(II), Ni(II), Cr(III) and Fe(III) complexes with amino acid and heterocyclic amines (CUKROWSKI *et al*., 2012).

Has been done reported on the investigation and antibacterial studies of binary and ligand complexes that mix of some transition metals with semicabazones/ thiosemicarbazones and amino acids or N-protected amino acids (Achar *et al*., 2018).

In view of the important biological activity of the thiosemicarbazones /semicarbazones, amino acids and their metal complexes, Complexes of transition metal(II), 1-12 of the type $[MCl(TSC)(L)]H_2O$, (where M= Co(II) and Cu(II); TSC = semicarbazone/ thiosemicarbazone ; L = amino acid (glycine, alanine) were formed by a stoichiometric ratio of M : TSC : L as 1: 1 : 1. These two different ligands incorporated with the metal ion were used in order to study the effect of the presence of two different types of ligands on the biological activity Cobalt

is a necessary element for human health maintenance; it is primarily linked to the function of cobalamin (vitamin B12), which indirectly regulates growth and DNA synthesis, as well as red blood cell formation and nervous

system health (Novakovic *et al*., 2006). In comparison to other metal compounds, the pharmaceutics of cobalt 17 compounds have gotten substantially less attention in the literature (He *et al* ., 2015;Hollo *et al*.,2014).

Schiff base metal complexes have been widely studied because they have industrial, antifungal, antibacterial, anticancer herbicidal applications(Sun and Haines.,1970) , anti-tubercular activities and chelating abilities which give it attracted remarkable attention(Gulab *et al*.,2018).

Metal complexes involving such compounds are of immense biological interest due to their part in the biological systems' trace metal ion exchange and transport mechanism (Ibrahim *et al*., 2019).

A series of metal complexes of Fe(II) and Zn(II) having the general composition [M(L)X] with benzyl bis(thiosemicarbazone) , is described. This simple and economical method is environmentally safe and requires less time. The [M(L)X] species of Fe(II) and Zn(II) probably catalyze the oxidation (Ibrahim *et al*., 2022). Typically, thiosemicarbazones form bonds with chelating ligands through the use of transition metal ions sulfur and hydrazine nitrogen.Transition metal complexes are effective catalysts in cross-coupling reactions, but their use as catalysts for aryl-aryl coupling has not been much studied. Mild and efficient aromatic couplings have been reported (Hassan *et al* ., 2019;Reddy., 2017).

Thiosemicarbazones (TSCs) are a class of Schiff base N and S donor ligands that are produced when thiosemicarbazides condense with various carbonyl compounds (Devagi *et al*., 2018;El-Remaily *et al*., 2024). The TSC ligands can interact with the metals as monoanionic or neutral species. Crystallography can identify these distinct binding modes because the deprotonated TSC form yields a formal C–S single bond of 1.71–1.80 Å, whereas the neutral form's C–S bond is a double bond of 1.67–1.72 Å (Kisa *et al*., 2019). The interest in the TSCs is driven by a potential significance in their biological applicability, due to their ability for DNA binding (Dorafshan et al., 2024), as anticancer (El-Sawaf *et al*., 2018), bactericidal (Feizi-Dehnayebi *et al*., 2021), fungicidal (Kathiravan et al., 2012), antitrypanosomal (Kaya *et al*., 2020) and antimalarial (Khan et al., 2014) agents.

In view of this introduction, this paper presents the preparation of two trivalent cobalt complexes, acronymed as **A1** and **A2** , produced via the reactions of cobalt(II) chloride hexahydrate with the bidentate thiosemicarbazid ligand and fructose , glucose ($C_6H_{12}O_6$). We now after the synthesis and detailed characterization of these cobalt complexes, report the antibacterial activities of these complexes and their ligands against a Gram +ve (S. aureus) and a Gram -ve (E. coli) bacterial species.

2. Materials and Methods

2.1 Chemicals and instruments

Cobalt (II) chloride , Glucose, and fructose, as well as thiosemicarbazide and sodium hydroxide were obtained from Laboratory Reagent Chemical Company, Chem King, BHD Chemical Company, and "Riedel-de Han" Chemical Companies. A distillation system was used to purify each and every solvent that was used . The calculated PXRD patterns were produced using the SHELXTL-XPOW program (Version 5.102, Bruker AXS, Germany) and single crystal reflection data. An infrared spectrum (4000 – 400 cm^{-1}) was carried out on a solid sample on a Unicam Mattson 1000 FTIR spectrometer. The electronic absorption spectra were recorded using a Shimadzu UV–2010 UV–Vis. doublebeam spectrometer. The antimicrobial activity of the tested samples for the complexes was determined using a modified Kirby- Bauer disc diffusion method (El-t Ashooret *et al*., 2023) . The test bacteria were grown in 100 microliters of 10 milliliters of fresh media until they were roughly 1^8 cells per milliliter. The growth was harvested and washed off with sterile normal saline. Using a surface counting technique, the average number of viable organisms per milliliter of saline suspension was calculated. After allowing the drops to dry for two hours at room temperature, the plates were incubated for twenty-four hours at 37^{o}C. Each slide's developed colony count was determined after incubation. The viable count of the stock suspension was calculated by multiplying the average number of colonies per drop (0.02 ml) by 50 and the dilution factor. This resulted in the number of colony-forming units per ml of suspension. Every time, a fresh suspension of stocks was made.

2.2 Excremental

2.2.1 Synthesis of [(thiosemicarbazid) (Fructose) Cobalt (II)] [Co(TSC)(FRU)(Cl)$_2$](A1):

Cobalt (II) Chloride [$CoCl_2.6H_2O$] (500mg , 2mmol) in 10 ml of ethanol was added to an equimolar quantity of thiosemicarbazide {CH_5N_3S} (192 mg , 2 mmol) in 10 ml of ethanol dropwise at room temperature with stirring. The temperature was gradually increased and the reaction mixture was reflux for 10 minutes, during that time the colour was turned to dark brown. After that aqueous solution of fructose (379mg, 2mmol) was added to the mixture. The reaction was reflux for in water bath for more than three hours. During that time the colour was observed brown. The complex was obtained by raising the pH of the reaction mixture by adding (0.01 mol) of KOH solution. The brown solid was separated from the cold solution by filtration. Then the solid compound was washed with cold water followed by a mixture of ethanol: water (1:1). The final sold was dried under vacuum, after purification of the product was acquired with (990 mg, 45%) (Scheme 1).

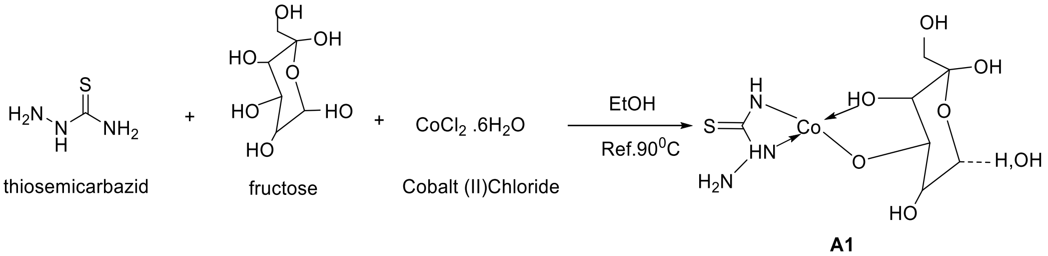

Scheme (1) preparation of [Co(TSC)(FRU)Cl$_2$] (A1)

2.2.2 Synthesis of [(thiosemicarbazid) (Glucose) Cobalt(II)] [Co(TSC) (GLU) $(Cl)_2$](A2):

By the same method described above this complex was synthesized. The preparation involved equimolar quantities of , Cobalt(II)Chloride , thiosemicarbazid {CH_5N_3S} and glucose with the ratio (1:1:1) and (amounts of 500mg, 192 mg and 379mg), (2mmol,2mmol,2mmol) respectively. The final brown product was collected and then purified with (981 mg ,45%) (Scheme 2).

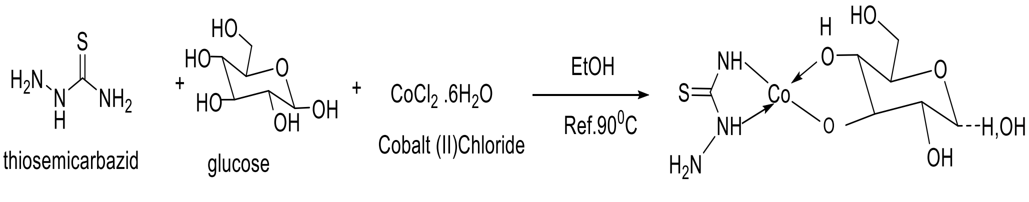

A2

Scheme (2) preparation of [Co(TSC)(GLU)] (A2)

2.2.3 Testing for antimicrobial properties

With a few minor adjustments, the cup-plate agar diffusion method was used to measure the antibacterial activity. Agar that had been incubated was divided into two groups, and 20 ml aliquots were placed into sterile Petri dishes. The agar was allowed to settle in each group's six cups, each of which had a diameter of 10 mm and was cut with a sterile corkscrew (No. 4). Each of the halves was designed for one of the test compounds. Separate Petri- dishes were created for the standard antibacterial chemotherapeutic agent. After removing the agar discs, 0.1 ml samples of each of the extracts and pure complexes were added to alternate cups using an adjustable volume microtiter pipette, and allowed to diffuse at room temperature for two hours. The plates were then incubated. in the upright position at 37°C for 24 hours.

The above procedure was repeated for different concentrations of the complexes and the standard antibacterial chemotherapeutic. Following incubation, the growth inhibition zones that resulted were measured and averaged in diameter (Ashoor *et al*., 2022).

2.2.4 Theoretical calculations

The Gaussian 09 program package (Rodic *et al*.,2012) was utilized for theoretical calculations with DFT methods. Thereafter, the B3LYP hybrid functional and the 6–311++G (d, p) basis set (El-t Ashoor *et al*., 2023) were employed for studying the quantum physical and chemical properties of the synthesized metal complexes using the atoms (H, C, N, F, O, and Cl) of the chelating agents(Gou *et al*., 2022). This is due to the fact that, when applied, this particular combination of functional and basis sets produced outcomes that closely matched the experiment in our earlier research.

GaussView 6.0 and Chemcraft software with a graphical user interface were used for all structural and spectroscopic illustrations (Shakoor *et al*., 2024).

3. RESULTS AND DISCUSSION

3.1. Electronic spectra insights

The solution electronic spectra of [Co(FRU)(HQ)] (A1) and [Co(GLU)(HQ)] (A2) are given in the Supplementary Information. From 200 to 800 nm, the UV-Vis. Spectra of the representative Co(II) complexes in the Ethanol solution were measured. The electronic spectrum of cobalt (II) complexes showed two bands observed in the range of 280-343 nm in the electronic spectrum of the ligand due to the intraligand $\pi \rightarrow \pi*$and n $\rightarrow \pi*$transitions. It displayed bands in the 400 and 442 nm ranges in the interim. The complex's Co(II) appears to have a square planar geometry, as indicated by the bands that appear below 472 nm.The bands appearing at 400 nm and 441 nm have been assigned to MLCT (metal-to- ligand charge transfer) (Suzen et al., 2017;TURI et al., 2012).

3.2. Analysis of vibrational spectra of A1 and A2

The FT-IR spectra of the two bidentate ligands and corresponding Co-based complexes provided significant indications of the bonding sites of saccharides and thiosemicarbazid ligands and the proposed assignment of complexes. The characteristic ν(N-H) stretching bands (located at 3300 cm^{-1}) and bending vibration bands (located at 1500 cm^{-1}) in the IR spectra of the two free ligands disappear after coordination with the Co ion. The ν(C=S) bands are found at 1598–1497 cm^{-1}, but the ν(C-N) vibrational bands in the two Co-based compounds are affected after complexation and are exhibited at around ∼1580 cm^{-1}. The band corresponding to the ν(C-O) vibration deprotonated and then moved to slightly higher energies in the complexes (from 1205 to 1276 cm^{-1}). Furthermore, the bands associated with Co-O and Co-N vibrations are observed in the range of 656–

497 cm^{-1}, as was previously reported(Yousef *et al*., 2014) . The plane and out-of-plane ring deformation modes were observed at 788 cm^{-1}, confirming coordination through the nitrogen atom of TSC with metal. As shown in Table 1 , Figure. 1 and Figure. 2 .

Table 1: FTIR Spectra of cobalt complexes

Complexes	*v*(N-H)	v(C=S)	v(Co-O)	v(Co-N)	v(Co-Cl)
[Co(TSC)(FRU)Cl_2] (A1)	3288.16	1496.84	1043	932.68	658.77
[Co(TSC)(GLU)Cl_2] (A2)	3250.55	1567.7	1048	931.81	678.97

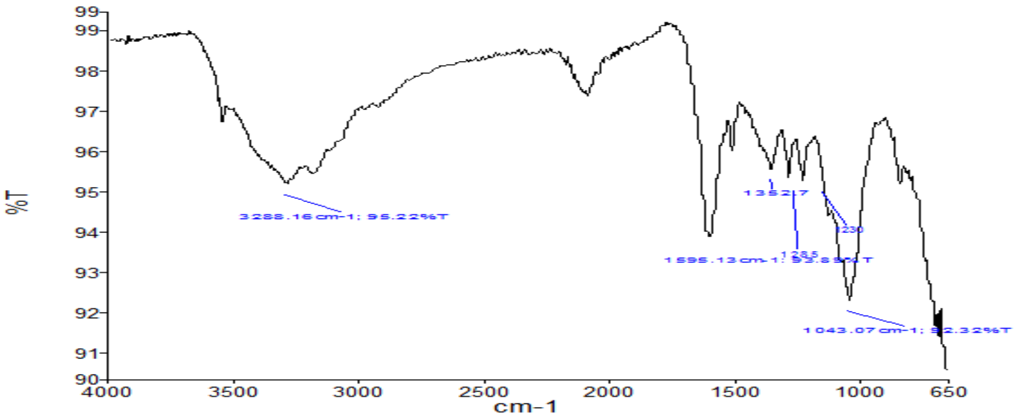

Figure 1: FTIR Spectra of Coblet complexe [Co(TSC)(FRU)Cl_2](A1)

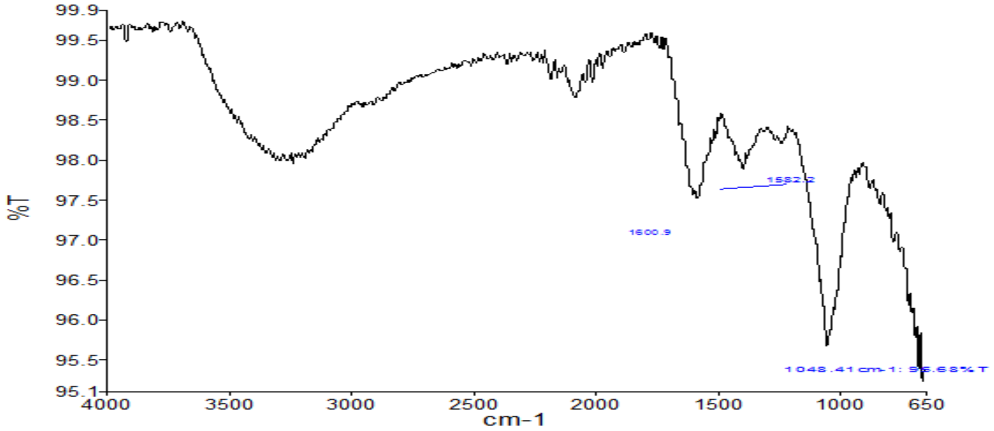

Figure 2: FTIR Spectra of Coblet complexe [Co(TSC)(GLU)Cl_2](A2)

3.3 Antibacterial Studies :

The antibacterial complexes were tested on the six species of bacteria including: (Staphylococcus aureus, Streptococcus spp., Escherichia coli, Klebsiella spp., Psuedomones spp. and Protues spp.) The complexes were under a variable concentration (0.1, 0.01, 0.001M). At the concentration of 0.001M , the complexes showed a positive influence on the six types of bacteria . The result is given in Table (2).

Table(2)Antibacterial Actibacterial Activitiesnin Concentration 0.001M

Complexes	*Staph. Aureus*		*Streptococcus* spp		*E. coli*		*Klebsiella* spp		*Pseudomonas* Spp		*Protues* spp	
	A	%	A	%	A	%	A	%	A	%	A	%
[Co(TSC)(FRU)Cl_2] (A1)	++	50%	++	50%	+	20%	++	40%	++	40%	+	20%
[Co(TSC)(GLU)Cl_2] (A2)	++	55%	++	60%	+	25%	+	30%	++	50%	+	20%

Percentage of Inhibition: Below 20% = (-) low active, 20% – 40% = (+) Active, 40% – 60% = (++) mildly active & 60% – 80% = (+++) moderately active, (80%, up) = (++++) highly active, *Activity

On all of the species of bacteria, but the complexes with fructose showed a positive influence on five of the species of bacteria, the result is given in (Table 3).

Table(3)Antibacterial Actibacterial Activitiesnin Concentration 0.01M

Staph. Aureus Complexes	*Staph. Aureus*		*Streptococcus* spp		*E. coli*		*Klebsiella* spp		*Pseudomonas* Spp		*Protues* spp	
	A*	%	A	%	A	%	A	%	A	%	A	%
[Co(TSC)(FRU)Cl_2] (A1)	++	60%	++	60%	+	25%	++	60%	+++	70%	+	25%
[Co(TSC)(GLU)Cl_2] (A2)	++	55%	++	60%	+	30%	+	30%	++	60%	+	20%

Percentage of Inhibition: Below 20% = (-) low active, 20% – 40% = (+) Active, 40% – 60% = (++) mildly active & 60% – 80% = (+++) moderately active, (80%, up) = (++++) highly active, *Activity

In concentration of 0.1M, complexes showed a highly positive influence on all types of bacteria. The results were given in (Table 4).

Table(4)Antibacterial Actibacterial Activitiesnin Concentration 0.1M

Complexes	*Staph. Aureus*		*Streptococcus* spp		*E. coli*		*Klebsiella* spp		*Pseudomonas* Spp		*Protues* spp	
	A*	%	A	%	A	%	A	%	A	%	A	%
[Co(TSC)(FRU)Cl_2] (A1)	+++	70%	++	60%	++	40%	++	60%	+++	70%	+	20%
[Co(TSC)(GLU)Cl_2](A2)	++	50%	++	65%	+	35%	+	30%	++	50%	+	20%

Percentage of Inhibition: Below 20% = (-) low active, 20% – 40% = (+) Active, 40% – 60% = (++) mildly active & 60% – 80% = (+++) moderately active, (80%, up) = (++++) highly active, *Activity

3.4 Computational

Density functional theory (DFT) calculations employing B3LYP, hybrid functional together with 6–311++G (d, p) basis set (Ashoor *et al.*, 2022) for atoms (H, C, N, F, O and Cl) of chelating agents were used to study the quantum physical and chemical properties of the synthesized metal complexes using the Gaussian 09 program package. This is because such a combination of functional and basis sets has been used and gave results that are in a good agreement with the experiment in our previous studies.

The transfer of electrons from the valence band to the conduction band is the source of UV-Vis light absorption. The distance between the valence and conduction bands, which was controlled by the doping agent ratio, is known as the energy band-gap. Quantum physical and chemical descriptors are pertinent in DFT and are used to establish how the structure, stability and reactivity of compounds relate to their biological activity.

In this work, Figure 3 and Figure 4 depict the typical plot of (Ahv)1/2 versus photon energy (hv) for indirectly allowed transitions, which is used to calculate the values of optical band gaps, e.g. using the Tauc plot, it is possible to determine the linear dependence between (Ahv)1/2 and photon energy. The indirect energy band gap is derived from the plot's linear region and is displayed in Figure 1. The results show that the indirect band gap values decrease from 0.54 to 0.24 eV for the compound [Co(TSC) (Fru)] (A1) and the compound [Co(TSC)(Glu)] (A2) respectively.

These results suggest that the changes in the [(Fru) (A1) ,(Glu) (A2)] bonding in two compounds network, such as the formation of NBOs, will result in changes in the absorption characteristics. This alteration explains the decrease in the optical band gap with the change in A1,A2 compounds.

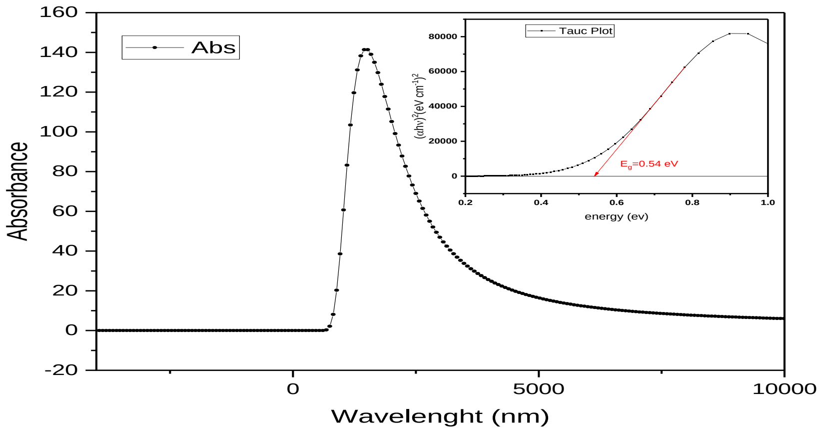

Figure 3: optical band gap energy use to determined the electrical and optical properties using Tauc Plot method for the compound [Co(TSC) (FRU)] (A1)

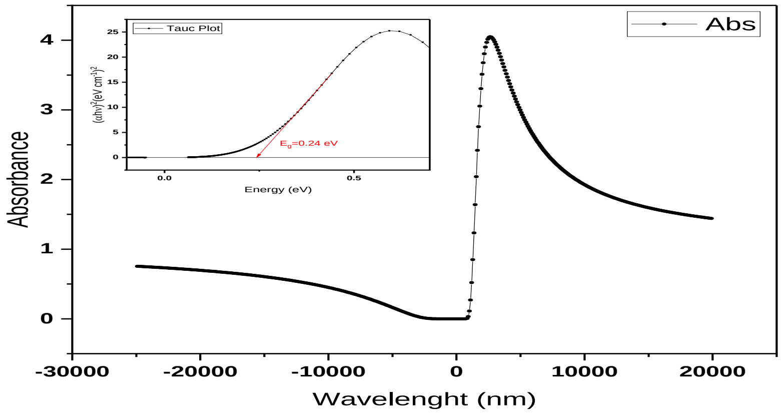

Figure 4:optical band gap energy use to determined the electrical and optical properties using Tauc Plot method for the compound [Co(TSC)(GLU)] (A2)

3.4.1. Optimized geometry of [Co(TSC)(FRU)] (A1) and [Co(TSC)(GLU)] (A2):-

The molecular geometries of the [Co(TSC)(FRU)] [Co(TSC)(GLU)] complexes, in their square planar metal coordination, are fully modeled. Table 5 reports the calculated bond lengths and angles, with the most significant coordination parameters displayed in Figure 5 and Figure 6 around the Cobalt (II) ion center. DFT computed structure of $[Pd(bipy)(acac)]^+$ (Feizi-Dehnayebi *et al*., 2021; El-t Ashoor *et al*., 2023) , leading to the distance variations, in good agreement with the literature though the different ligands and ion metals were involved.

Notably, the DFT optimization geometry reveals that the [Co(TSC)(FRU)] complex model has tetrahedral coordination around the metal (Figure 5), in contrast to the [Co(TSC)(GLU)] square coordination analogous (Figure 6). Indeed, as shown on Figure 5 , the Co(II) ion metal in the [Co(TSC)(FRU)] (**A1**) complex is bonded to the N, N-atoms of thiosemicarbazid , and O, OH of Fructose ligands, with bond length values for Co-N_1 and Co-N_2 of 1.729 (1.562 Td - 1.897 sq), and 1.846 (1.783 Td – 1.910 sq) ˚A, respectively, and average Co–O_1, Co-O_2 of 1.439 (1.123 Td- 1.748sq) ˚A. These bond distances are computed lower on average for the Fructose molecule in comparison to the Glucose Td geometry congener given between parentheses. The computed bond angles in the square complex [Co(TSC)(FRU)] in comparison with those given between parentheses and obtained for the [Co(TSC)(Glu)] Td analogous, i.e., O_1-Co-O_2 93.19 °(91.94), N_1-Co-N_2 72.74 °(70.14 °), C_2-O_1- Co 118.21 °(117.01 °), and O_1-C_2-C_3 95.04 °(92.84 °), clearly differentiate the two sugars, sustaining the Tetrahedral geometry structure of the [Co(TSC)(Glu)]. It is noteworthy that for the [Co(TSC)(FRU)] model , the optimized square geometry is at only 3 kcal/mol higher energy than the Td analogous.

Table (5) Selected bond lengths and angles in[Co(TSC)(FRU)] (A1) and [Co(TSC)(GLU)] (A2)

Complexes				Ref.38			
Bond	lengths (°A)	Fragment	Angles	Bond	lengths (A°)	Fragment	Angles
Co-O_1 (A1)	1.748	O_1-Co-O_2(A1)	93.194	Co-O_1 (A1)	1.980	O_1-pd_1 -O_2	93.38
Co-O_2 (A1)	1.619	N_1-Co-N_2(A1)	72.740	Co-O_2(A1)	1.980	N_1-pd_1 -N_2	74.83
Co-N_1 (A1)	1.897	C_2-O_1-Co(A1)	118.219	Co-N_1 (A1)	2.020	C_2-O_1-pd_1	120.955
Co-N_2 (A1)	1.910	O_1-C_2-C_3(A1)	95.048	Co-N_2 (A1)	2.017	O_1-C_2-C_3	93.562
N_1-C_1 (A1)	0.825	C_3-O_2-Co(A1)	118.418	N_1-C_1 (A1)	1.28	C_3-O_2-pd_1	120.955

N_2-C_1 (A1)	0.825	O_2-C_3-C_2(A1)	95.921	N_2-C_1 (A1)	1.280	O_2-C_3-C_2	93.562
O_1-C_2 (A1)	1.276	Co-N_1-C_1(A1)	125.216	O_1-C_2 (A1)	1.075	Co-N_1-C_1	126.072
O_2-C_3 (A1)	2.148	O_1-Co-O_2(A2)	91.940	O_2-C_3 (A1)	1.074	O_1-pd_1 -O_2	93.38
Co-O_1 (A2)	1.123	N_1-Co-N_2(A2)	70.140	C_2-C_3 (A1)	1.474	N_1-pd_1 -N_2	74.83
Co-O_2 (A2)	1.266	C_2-O_1-Co(A2)	117.019	Co-O_1 (A2)	1.980	C_2-O_1-pd_1	120.955

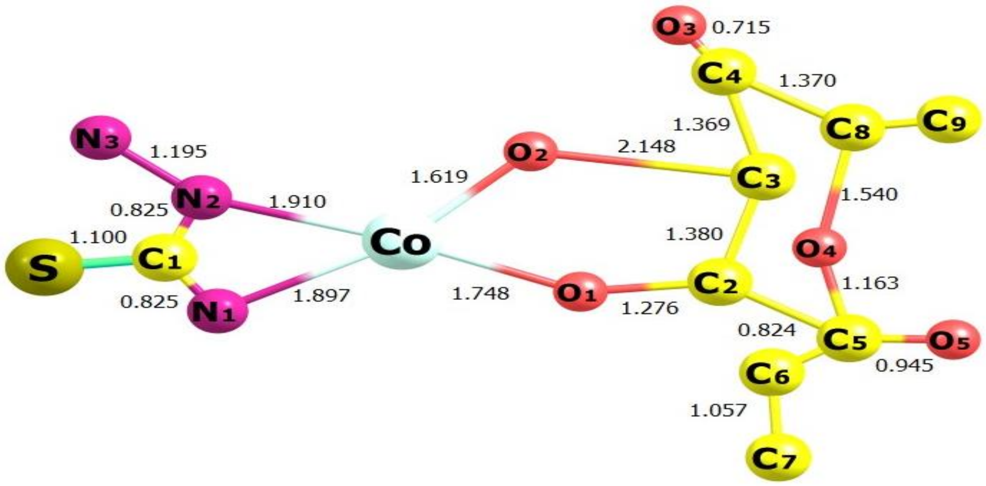

Figure 5: DFT/B3LYP/TZP optimized geometry of the [Co(TSC)(FRU)] (A1) model complexes.

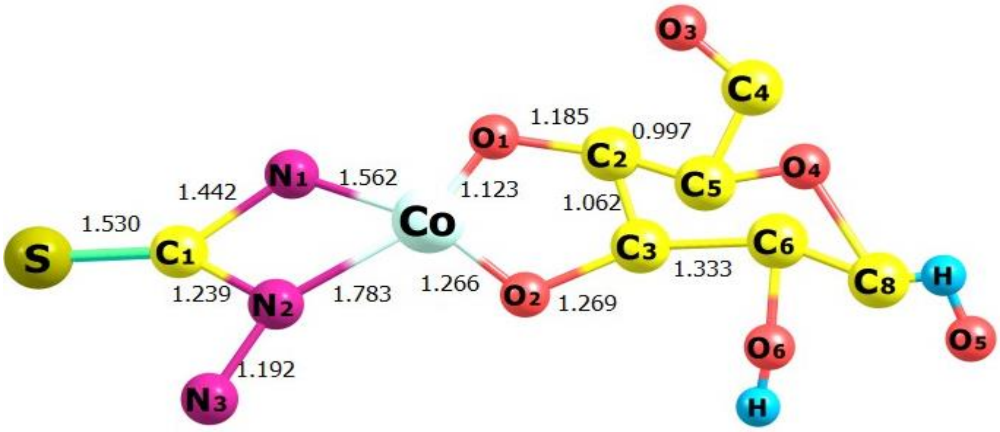

Figure 6: DFT/B3LYP/TZP optimized geometry of the [Co(TSC)(GLU)] (A2) model complexes.

Conclusion

Compounds [Co(TSC)(FRU)] (A**1**) and [Co(TSC)(GLU)] (A**2**) were combined and described experimentally using spectroscopic methods. Theoretical calculations were performed on complexes **A1** and **A2**. Preliminary publications demonstrated a notable degree of harmony between the calculated theoretical geometries and the physicochemical and computational studies that were discussed. Square planar geometry is proposed for the Co (II) complex in the case of [Co(TSC)(FRU)] (**A1**), whereas complex [Co(TSC)(GLU)] (A**2**) showed tetrahedral coordination around the metal ion, which could be due to greater flexibility around the metal ion. In the case of saccharides, the ligands are bidentate through two nitrogens of the thiosemicarbazide with the oxygen of hydroxide in the case of saccharides. Figure 3 and Figure 4 show the gap energy via output DFT calculation of these complexes. The complexes under investigation demonstrated strong activity against the majority of bacteria and are effective antibacterial agents.

References

Abdel-Rahman, L. H., Abu-Dief, A. M., Moustafa, H., & Abdel-Mawgoud, A. A. H. (2017). Cr (III), VO (II), and Ni (II) Chelates Incorporating Tri-dentate Imine Ligand for DNA Interaction, Antimicrobial, Anticancer Activities and Molecular Docking Studies.

Achar, G., Agarwal, P., Brinda, K. N., Małecki, J. G., Keri, R. S., & Budagumpi, S. (2018). Ether and coumarin–functionalized (benz) imidazolium salts and their silver (I)–N–heterocyclic carbene complexes: Synthesis, characterization, crystal structures and antimicrobial studies. *Journal of Organometallic Chemistry*, *854*, 64-75.

Ashoor, S. E. T., Abokhater, R. A., & Treina, N. B. (2022). Synthesis, DFT Study and the Biological Activity of 8-Hydroxyquinoline Zirconium (IV) Complexes. *European Journal of Applied Sciences*, *10*(4), 726-737.

Berto, S., Alladio, E., Daniele, P. G., Bono, A., Laurenti, E., Sgarlata, C., ... & Nurchi, V. M. (2019). Oxovanadium (IV) complexes with newly synthetized kojic acid derivatives. In *ISMEC 2019* (pp. 42-43). University of Debrecen.

ÇAKMAK, R., DAĞ, B., & YAŞAR, F. (2013). New Schiff Base Ligand Derived From 4-aminoantipyrine: Synthesis and Spectroscopic Characterization. In *Chair of the Conference* (Vol. 104, No. 213, p. 106).

CUKROWSKI, I., SARKAR, A., van ASWEGEN, A., & LILES, D. (2012). Protonation sequence of zoledronic acid: a DFT and QTAIM study. *Maria Amélia Santos, Editor*, *76*, 120-126.

Deodware, S. A., Barache, U. B., Dhale, P. C., Gaikwad, K. D., Shivamallu, C., Ubale, P. A., ... & Glossman-Mitnik, D. (2022). In vitro anticancer screening, molecular docking and antimicrobial studies of triazole-based Nickel (II) metal complexes. *Molecules*, *27*(19), 6548.

Devagi, G., Dallemer, F., Kalaivani, P., & Prabhakaran, R. (2018). Organometallic ruthenium (II) complexes containing NS donor Schiff bases: Synthesis, structure, electrochemistry, DNA/BSA binding, DNA cleavage, radical scavenging and antibacterial activities. *Journal of Organometallic Chemistry*, *854*, 1-14.

Dorafshan Tabatabai, A. S., Dehghanian, E., Mansouri-Torshizi, H., & Feizi-Dehnayebi, M. (2024). Computational and experimental examinations of new antitumor palladium (II) complex: CT-DNA-/BSA-binding, in-silico prediction, DFT perspective, docking, molecular dynamics simulation and ONIOM. *Journal of Biomolecular Structure and Dynamics*, *42*(10), 5447-5469.

El-Remaily, M. A. E. A. A., Aboelez, M. O., Ezelarab, H. A., Selim, H. M. R. M., Taha, E. A., Mohamed, S. K., ... & Kamel, M. S. (2024). Guanidine dicycloamine-based analogs: green chemistry synthesis, biological investigation, and molecular docking studies as promising antibacterial and antiglycation leads. *Molecular Diversity*, 1-23.

El-Sawaf, A. K., El-Essawy, F., Nassar, A. A., & El-Samanody, E. S. A. (2018). Synthesis, spectral, thermal and antimicrobial studies on cobalt (II), nickel (II), copper (II), zinc (II) and palladium (II) complexes containing thiosemicarbazone ligand. *Journal of Molecular Structure*, *1157*, 381-394.

El-t Ashoor, S., Abokhater, R. A., Belkhiri, L., & Gadir, S. A. (2023). Spectroscopy and DFT studies on Cr (III) complexes with saccharides, 8-hydroxyquinoline and their biological activity. *Journal of Molecular Structure*, *1281*, 135134.

Feizi-Dehnayebi, M., Dehghanian, E., & Mansouri-Torshizi, H. (2021). Synthesis and characterization of Pd (II) antitumor complex, DFT calculation and DNA/BSA binding insight through the combined experimental and theoretical aspects. *Journal of Molecular Structure*, *1240*, 130535.

Gou, Y., Jia, X., Hou, L. X., Deng, J. G., Huang, G. J., Jiang, H. W., & Yang, F. (2022). Dithiocarbazate–FeIII,− CoIII,− NiII, and− ZnII complexes: Design, synthesis, structure, and anticancer evaluation. *Journal of Medicinal Chemistry*, *65*(9), 6677-6689.

Gulab, H., Shah, Z., Mahmood, M., Shah, S. R., Ali, S., Iqbal, M., ... & Khan, S. A. (2018). Synthesis, characterization and antibacterial activity of a new calcium complex using sodium 2-mercaptobenzothiazole and 1, 10-phenanthroline as ligands. *Journal of Molecular Structure*, *1154*, 140-144.

Hassan, S. S., & Gomha, S. M. (2019). Novel functionalized thiosemicarbazone ligands and their Pd (II) complexes: synthesis, characterization, antibacterial and cytotoxic activities. *Chemical Papers*, *73*, 331-344.

He, D., Jian, W., Liu, X., Shen, H., & Song, S. (2015). Synthesis, biological evaluation, and structure–activity relationship study of novel stilbene derivatives as potential fungicidal agents. *Journal of agricultural and food chemistry*, *63*(5), 1370-1377.

Holló, B., Rodić, M. V., Vojinović-Ješić, L. S., Živković-Radovanović, V., Vučković, G., Leovac, V. M., & Szécsényi, K. M. (2014). Crystal structure, thermal behavior, and microbiological activity of a thiosemicarbazide-type ligand and its cobalt complexes. *Journal of Thermal Analysis and Calorimetry*, *116*, 655-662.

Ibrahim, A. B., Farh, M. K., & Mayer, P. (2019). Synthesis, structural studies and antimicrobial evaluation of nickel (II) complexes of NNS tridentate thiosemicarbazone based ligands. *Applied Organometallic Chemistry*, *33*(7), e4883.

Ibrahim, A. B., Mahmoud, G. A. E., Cordes, D. B., & Slawin, A. M. (2022). Pb (II) and Hg (II) thiosemicarbazones for inhibiting the broad-spectrum pathogen Cladosporium sphaerospermum ASU18 (MK387875) and altering its antioxidant system. *Applied Organometallic Chemistry*, *36*(8), e6798.

Kathiravan, M. K., Salake, A. B., Chothe, A. S., Dudhe, P. B., Watode, R. P., Mukta, M. S., & Gadhwe, S. (2012). The biology and chemistry of antifungal agents: a review. *Bioorganic & medicinal chemistry*, *20*(19), 5678-5698.

Kaya, B., Akyüz, D., Karakurt, T., Şahin, O., Koca, A., & Ülküseven, B. (2020). Cobalt (II)/(III) complexes bearing a tetradentate thiosemicarbazone: Synthesis, experimental and theoretical characterization, and electrochemical and antioxidant properties. *Applied Organometallic Chemistry*, *34*(11), e5930.

Khan, S. A., Asiri, A. M., Al-Amry, K., & Malik, M. A. (2014). Synthesis, characterization, electrochemical studies, and in vitro antibacterial activity of novel thiosemicarbazone and its Cu (II), Ni (II), and Co (II) complexes. *The Scientific World Journal*, *2014*(1), 592375.

Kısa, D., Korkmaz, N., Taslimi, P., Kardağ, A., & Tekin, Ş. (2019). The effect of coordination compounds on carbonic anhydrase (CA) activity. International Eurasian Conference on Biological and Chemical Sciences.

Novaković, S. B., Bogdanović, G. A., & Leovac, V. M. (2006). Transition metal complexes with thiosemicarbazide-based ligands. Part L. Synthesis, physicochemical properties and crystal structures of Co (II) complexes with acetone S-methylisothiosemicarbazone. *Polyhedron*, *25*(5), 1096-1104.

Reddy, A. (2017). *The Synthesis of Functionalized Glycosides: Coordination Chemistry, Antiparasitic Activity, Precursors to Conformationally Constrained Macrocyclic Architectures and Photophysical Properties*. National University of Ireland, Maynooth (Ireland).

Rodić, M. V., Leovac, V. M., Jovanović, L. S., Vojinović-Ješić, L. S., Divjaković, V., & Češljević, V. I. (2012). Transition metal complexes with thiosemicarbazide-based ligands: Part 59. Synthesis, structures and electrochemical properties of cobalt (III) complexes with 2-acetylpyridine S-methylisothiosemicarbazone. *Polyhedron*, *46*(1), 124-132.

Shakoor, A., Fareed, G., Ahmad, I., Elhenawy, A. A., Khan, M., Fareed, N., ... & Ibrahim, M. (2024). Exploring the Anti-Diabetic Activity of Benzimidazole Containing Schiff Base Derivatives: In Vitro α-amylase, α-glucosidase Inhibitions and In Silico Studies. *Journal of Molecular Structure*, 140136.

Sun, K. K., & Haines, R. A. (1970). Studies of cobalt (III) complexes of thiosemicarbazide. *Canadian Journal of Chemistry*, *48*(15), 2327-2333.

Süzen, Y., Metinoğlu, S., & Ashoor, S. E. T. (2017). Synthesis of new bis-bidendate N/O spiro-bino-spiro-cyclotriphosphazenes: Structural investigations and DFT studies. *Phosphorus, Sulfur, and Silicon and the Related Elements*, *192*(1), 118-128.

TURI, I., & SÓVÁGÓ, I. (2012). Mixed transition metal complexes of model peptides related to the metal binding site of prion protein. *Maria Amélia Santos, Editor*, *48*, 2.

Yousef, T. A., El-Gammal, O. A., Ahmed, S. F., & El-Reash, G. A. (2014). Structural, DFT and biological studies on Co (II) complexes of semi and thiosemicarbazide ligands derived from diketo hydrazide. *Journal of Molecular Structure*, *1076*, 227-237.